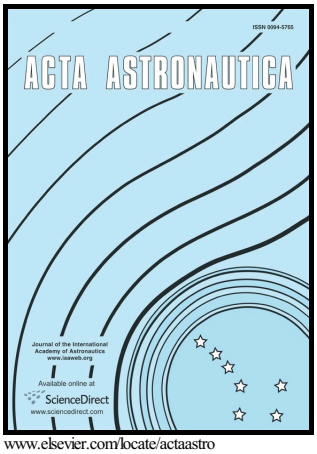

www.elsevier.com/locate/actaastro

Experimental Research on Tape Spring Supported Space Inflatable Structures

Andrew J. Cook, Scott J.I. Walker

PII: S0094-5765(15)00387-2
DOI: http://dx.doi.org/10.1016/j.actaastro.2015.10.016
Reference: AA5579

To appear in: *Acta Astronautica*

Received date: 2 January 2015
Revised date: 10 September 2015
Accepted date: 22 October 2015

Cite this article as: Andrew J. Cook and Scott J.I. Walker, Experimental Research on Tape Spring Supported Space Inflatable Structures, *Acta Astronautica,* http://dx.doi.org/10.1016/j.actaastro.2015.10.016

Suggested reviewers:

Michael Lou Email: Michael.c.lou@jpl.nasa.gov

Kevin Brayley Email: Unknown
First author of "Bending response of externally reinforced, inflated, braided fabric arches and beams"
Corresponding author email: william.davids@umit.maine.edu (W.G. Davids)

Experimental Research on Tape Spring Supported Space Inflatable Structures

Andrew J. Cook* and Scott J.I. Walker†
University of Southampton, Southampton, Hampshire, UK, SO17 1BJ

This paper presents experimental research that continues the development of inflatable hybrid structures for space applications. Inflatables provide a concept with much scope for further incorporation into the structures of future spacecraft. They offer considerable savings in mass and stowed volume for spacecraft, providing possible reductions in satellite costs. Existing boom configurations make use of inflatables including solar arrays and the NGST sunshield. However these typically soft systems could be improved by incorporating tape springs as structural stiffeners along the length of the boom, creating hybrid structures. This research builds on previous experimental work undertaken at the University of Southampton looking at cantilever inflatable and hybrid booms.

The focus of this research is to identify the structural performance improvement of adding tape springs to cantilever inflatable booms. This is achieved by tip deflection testing to determine the bending moment and rigidity performances of these structures allowing a comparison between the two technologies. Several hybrid booms are created and tested in various orientations to identify the optimal tape spring effectiveness. It was found that adding a pair of tape springs will increase stiffness of the hybrid structure by up to 4.9 times for an increase of 2.4 times the boom mass.

* Corresponding Author. Postgraduate Research Student, Astronautics Research Group, Highfield Campus, University of Southampton SO17 1BJ. Tel.: +44 7873323381
Email address: ac1705@soton.ac.uk
† Lecturer in Aerospace structures, Astronautics Research Group, Highfield Campus, University of Southampton SO17 1BJ.

Nomenclature

L	=	Load
M	=	Moment
M_{fail}	=	Moment causing boom failure
M_{max}	=	Maximum achievable moment
Mw	=	Moment causing initial wrinkling on the boom
M_{+}^{max}	=	Maximum tape spring opposite sense bending moment
M_{-}^{max}	=	Maximum tape spring equal sense bending moment
M_{+}^{*}	=	Tape spring opposite sense steady state bending moment
M_{-}^{*}	=	Tape spring equal sense steady state bending moment
p	=	Pressure
R	=	Radius of curvature
r	=	Radius
t	=	Thickness
α	=	Angle of embrace
σ_H	=	Hoop boom stress
σ_L	=	Longitudinal boom stress

1. Introduction

INFLATABLE structures offer savings in mass and stowage volume and thus reduce the cost of launch [1]; however, they are often poor in structural stiffness. This research investigates the use of hybrid structures for inflatable booms, focusing on maintaining the mass advantages of gossamer structures while increasing the structural performance of the booms.

It is intuitive that inflatables can create large space structures that would otherwise be difficult to send into orbit from a single launch. TransHab [2], Genesis I and II [3], and Bigelow's Space Station Alpha [4] are examples of a simple and cost effective way to create large structures for human habitation. Other examples include inflatable booms used instead of traditional support elements to mount equipment, such as solar arrays [5][6][7], sunshades

[8], and solarsails [9], that must be stowed during the launch phase. These can decrease the complexity of the mechanisms and deployment systems, reducing both the cost of manufacture and the mass and volume.

Significant research has taken place on inflatable booms with early work by Leonard et al (1960) [10] on inflatable tubes showing

$$M_{max} = \pi p r^3, \tag{1}$$

where p and r are boom inflation pressure and radius respectively. M_{max} is the maximum bending moment the boom can achieve creating large tip deflections as the boom collapses. Further more detailed analytical models have been developed such as the moment-deflection response of an isotropic inflatable boom using Euler-Bernoulli beam theory by Comer and Levy (1963) [11]. Webber (1982) [12] considered a similar setup performing static analysis on an inclined plane considering both bending and torsional responses with experimental verification demonstrating

$$M_{\mathrm{W}} = \frac{\pi p r^3}{2}, \tag{2}$$

where M_W is the incipient wrinkling moment of the inflatable boom. Main et al. (1995) [13] has extended this to include orthotropic materials and considered the varying planar material properties of fabrics. More recently Veldman (2005) [14] has also considered anisotropic inflatable beams and conducted finite element analysis to create inflatable booms using shell elements to investigate boom bending and torsion [15] similarly to Webber (1982). The research showed good correlation to the experimental and theoretical results. However there was increasing divergence between results at increased pressures. Experimental research by Thomas and Wielgosz (2004) [16] has shown highly inflated booms create pressure stiffening effects affecting the load-deflection response and increasing the load capacity of booms. Davids (2007) [17] formalised this by incorporating work done by pressure from deformation induced volume changes to a Timoshenko finite beam element model. This has confirmed both experimentally and analytically [18] the peak moment capacity of highly pressurised inflatable booms is greater than $2M_w$. This area of research continues to be developed across a variety of permutations including non-constant boom radius, arches and toroidals under various loading conditions, and further understanding of boom wrinkling behavior [19][20][21][22].

The structural performance of a boom can be judged by the stiffness and the loading capacity against the mass of the structure. To improve the structural performance of airbeams Brayley et al. (2012) [23] have investigated reinforcing sections of inflatable booms and aches along their length. This was achieved using four polyester straps bonded to the surface of the structure and have developed a 2D finite element model incorporating strap demonstrating a good correlation to their experimental results. Although a small stiffening effect was seen in the post buckling state, a key limitation of this reinforcement is the straps remain unable to sustain compressive loads. Work by Lou et al (2000) [24] shows the possibility of using carpenter tape springs with inflatable booms. The tape springs can sustain compressive loads and creates a hybrid structure able to increase the stiffness and buckling bending moment under axial compression while maintaining the advantages of gossamers.

Tape springs are defined as thin metallic strips with an initially curved cross-section [25]. They are a simple single element component that are easy to manufacture and lightweight. Tape springs exhibit non-permanent deformation while also storing strain energy in the buckled state allowing them to be simply stowed and able to drive deployment. In addition they have a relatively high buckling moment making them ideal as a structural element combined with an inflatable boom. Space industry developments including solarsail designs [26][27][28] utilize this technology to create lightweight flat surface arrays in addition to continued research using tape springs as hinges for self-deployable structures [25][29][30]. Combining inflatable and tape spring technologies creating a hybrid structure could increase the structural performance of a boom whilst also reducing cost of deployment. Although this technology has been previously considered for larger applications [ref lou] this scalable technology could be applied to small satellite low cost missions. An example of which would be to provide a low cost approach for deorbiting cube satellites in LEO utilizing the aerodynamic drag by deploying a surface array as suggested by Maessen (2007) [40]

Previous hybrid boom research by Walker et al (2011) [31] shows that the buckling bending moment achieved by a 350 g/m cantilever inflatable boom is 19 Nm at 103.4 kNm^{-2} and increased to 25 Nm when adding two opposed tape springs vertically aligned to the applied tip load. This was for a 50 mm radius inflatable boom, 0.6 m long. The steel tape springs had a flattened width of 25 mm with an additional mass of 21.5 g/m per tape. Other new boom technologies include the omega carbon fiber boom [26][32], which sets a bench mark buckling bending moment of 40 Nm for a boom mass of 62 g/m, and the NGST sunshield [8], which uses inflatable booms of 290.5 g/m that initially withstand 29 Nm at 22.1 kNm^{-2}. This is increased to 69 Nm when the heat curable composite is rigidized.

The aim of this paper is to provide the basis of hybrid boom structural performance trends with a detailed account of the experimental setup, procedure and test results. This paper outlines the current structural capabilities of a hybrid structure, adding tape springs as stiffeners to an inflatable cantilever boom, furthering the previous work set out by Walker et al. (2011) [31]. The tape springs will be tested in various configurations around the circumference of the boom to identify the effects of the change in the second moment of area, in order to maximize the boom performance. The experimental accuracy is improved from previous work by Walker et al (2011) [31] by using a refined method to achieve a better understanding of the inflatable and hybrid booms. From this future studies will aim to model these structures analytically and investigate the multitude of tape spring placement permutations.

2. Background

To determine the structural performance of the inflatable and hybrid booms, experimental tip deflection testing was undertaken to establish the change in stiffness and maximum bending moment before the booms fail. The mass of the booms was also measured to determine the effective performance increase generated by the use of tape springs.

The material selection for the hybrid booms is based upon cost, supply, and material properties. Inflatable space applications commonly use advanced materials such as Kevlar[15] or Vectran fabrics for their superior performance and suitability to the space environment. However for an initial investigation to establish hybrid boom trends, Nylon fabric was chosen because it is one of the strongest 'off the shelf' fabrics at a low cost. Nylon is a cheap alternative that has previously been used in space applications [24,39] and has sufficient structural properties for an inflatable boom. The materials used to manufacture the booms were 0.20 mm thick Ripstop Nylon Fibremax 94 [33], and a 0.5 mm thick rubber latex to provide an airtight bladder. The Nylon creates the outer shell which provides the rigidity of the boom while the bladder inflates taking the shape constrained by the Nylon. The Nylon outer tube was manufactured in two pieces; the boom length and the circular boom tip. These were stitched together by nylon thread in a simple single stitch at the end of the boom length, and closed to form a tube by a seam running the length of the boom. A dummy seam was also stitched into the boom length on the opposite side to give a symmetric profile and to match previous experiments by Lou et al (2000) [24]. The bladder was similarly constructed in two pieces and bonded with a water based adhesive called Copydex. An aluminum disc of 52 g with several small holes in its

centre was placed between the bladder and Nylon inside the tube. This was to stop the boom ballooning, giving a fixed flat end to the boom from which length and deflections were accurately measured. It also provided a loading point to apply the bending moment, where a 3 mm nylon cord was threaded through the disc and attached to the suspended weights. This allowed the load to be applied in the neutral axis at the boom tip, ensuring neither top nor bottom surface was preferentially loaded. The Nylon fabric was selected as being the most suitable from a range of materials, considering a number of parameters, including density and strength, as stated in Walker et al (2011) [31].

It is also important to consider the anisotropic behavior of fabrics. Fabrics are manufactured by longitudinal yarns (known as the warp direction) that are interwoven by transverse yarns (known as the fill direction). As a result, fabrics tend to be stronger in the warp direction and weakest in the bias direction (45^0 between warp and fill). This is an important consideration as the material properties will determine the structural performance of an inflatable boom including the maximum operating pressure, and input values for future computational and theoretical models. This is calculated from tensile testing of the fabric.

Tensile testing of the Nylon was undertaken in various configurations to identify the strongest and weakest orientations of the material. It is well known that pressure vessels are twice as strong longitudinally as in the hoop direction. It can therefore be expected the maximum pressure an inflatable boom can maintain prior to tip loading is determined by the hoop stress given as

$$\sigma_H = \frac{pr}{t} \text{ (Ref. [34])}, \tag{3}$$

where t is the thickness of the Nylon fabric. The maximum operating pressure may also be dependent on the applied bending moment with the resultant longitudinal boom tensile stress acting on the fabric. This is dependent on the varying ultimate tensile stresses (UTSs) of the orthotropic Nylon fabric. The UTS can be used to calculate the hoop and longitudinal stresses acting on the booms and was measured through tensile testing of the material. As seams run along the length and tip of the boom due to manufacturing, it was also important to find the UTS of the stitching joining the two Nylon pieces together. The Nylon fabric was tested in the warp and fill orientations with each having both stitched and non-stitched specimens. A further test of the material in the bias direction without a stitch was also conducted resulting in 5 sets of tests.

Fig. 1 Setup of the nylon tensile testing.

Figure 1 shows the setup of the tensile testing and follows the same procedure as Walker et al. (2011) [31], to comply with the British standard test procedures for aerospace textiles [35]. Each specimen was made to dimensions 200 × 50 mm of which 50 mm was gripped from both sides of the Nylon leaving a free length of 100 mm to be tested. In the case of stitched specimens, each end had a 5 mm overlap and was joined using a simple 1.5 mm stitch, in the same way as the boom seams. Each specimen type was subjected to 3 repeat tests and was placed under 5 mm per minute strain rate until maximum tensile stress was achieved and the specimen failed.

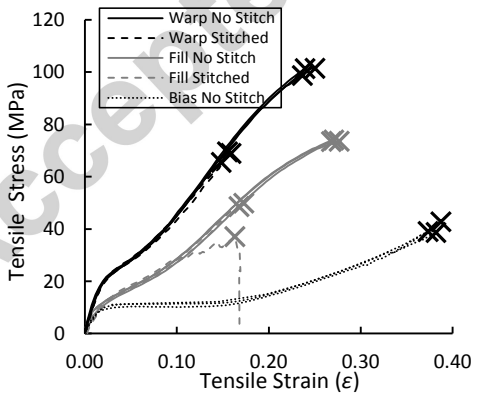

Fig. 2 Uniaxial tensile $\sigma - \varepsilon$ data of the Fibremax 94 Nylon fabric.

Table 1 Ultimate tensile stress of Fibremax 94.

Material configuration		Ultimate tensile stress (MNm^{-2})		
		Test 1	Test 2	Test 3
Warp	No stitch	101.5	98.7	101.3
	Stitch	69.5	68.9	65.4
Fill	No stitch	74.1	73.4	73.6
	Stitch	37.0	48.6	50.1
Bias	No stitch	38.6	39.1	42.8

Figure 2 displays the stress – strain data for the warp, fill and bias orientated specimens where an 'X' marks the failure point. The response of one 'Fill stitched' specimen is an anomaly and is caused by a gradual unzipping of the stitch at one edge from 30 MPa and a resulting lowered ultimate tensile strength (UTS) of 37 MPa. This cannot happen in the inflatable boom application as the seam ends are wrapped around the inner plate and overlapped by the tip end stitching forcing the stitch to fail similarly to the remaining specimens. The fabric behaves nonlinearly similarly to the polyurethane-coated nylon fabric reported by Glaser and Caccese (2013) and is caused by several macro-scale fabric mechanisms. The sequential regions of similar stiffness relate to inter-fibre frictional effects, yarn decrimping and yarn extension respectively in the fill and warp directions. In the biased direction the mechanisms are altered to inter-yarn frictional effects, yarn slippage and shear locking successively [refs].

Table 1 shows the UTS of each specimen type mounted in each orientation, showing the maximum achievable stress to be over 98 MNm^{-2} in the warp direction without any stitching. However, this is reduced to 65 MNm^{-2} when there is a stitch in the specimen. In comparison to the fill direction the fabric is over 30 stronger in the warp direction when considering the stitched specimens. Therefore by considering$\sigma_H = 2\sigma_L$, where σ_L is the longitudinal boom stress, and Eqn. (1) the structural capacity is maximised through its operating pressure by manufacturing the boom with the warp yarns in the hoop direction. The UTS of the stitch specimens predict the boom will fail from over pressurization in the hoop direction. This was demonstrated by 3 pressurisation failure tests where the inflatable booms burst along the hoop seam. Figure 3 shows a boom failure from over pressurisation where the initially 50 mm radius booms failed at 152, 165 and 172 kNm^{-2}. To ensure boom durability and accommodate additional longitudinal tensile stress under tip loading conservative test pressures of 69 kNm^{-2} (10 psig) and 103 kNm^{-2} (15 psig) were selected. The maximum radius due to inflation at these pressures was 53 and 54.5 mm for 69 and 103 kNm^{-2} respectively and constrained to 50 mm at the boom root and tip. A maximum radius of 56 mm at 159 kNm^{-2} was achieved prior to boom failure.

Formatted: Font color: Auto

Fig. 3 Over pressurisation failure at 165 kNm^{-2} of a 50 mm radius inflatable fabric boom.

The steel tape springs used to create the hybrid structure can be defined by three geometric parameters; Radius of curvature, *R*, thickness, *t*, and angle of embrace, α. These are shown graphically in Fig. 4 [25], and have the following properties; R = 15 mm, t = 0.11 mm, α = 1.67 rad, and a mass of 21.25 g/m length.

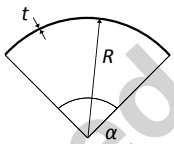

Fig. 4 Cross sectional tape spring parameters.

Tape springs use their curvature to enable them to resist buckling when being subjected to a moment normal to the centre of the tapes' width. Depending on the direction of the applied moment, the tape spring will buckle producing a longitudinal radius of curvature either on the same side or the opposite side to the initial transverse radius of curvature. These folds are known as two-dimensional equal- and opposite-sense bends respectively. Depending on the tape spring orientation the maximum bending moment the tape spring can achieve will vary. It is known from previous research that a tape spring buckles through a snap-through mode in the opposite sense bend, and a torsional mode for an equal sense bend [36]. This results in a higher buckling moment magnitude for an opposite sense bend (M_{+}^{max}) compared to an equal sense bend (M_{-}^{max}). This is shown in Fig. 5, which also shows that after buckling

there is a steady state bending moment (M^*_-, M^*_+) irrespective of further rotation. Simple experimental cantilever tip deflection tests of five 400 mm tape springs determine an average peak bending moment of 93 ±2 Nmm and 813 ±35 Nmm for equal (M^{max}_-) and opposite (M^{max}_+) sense bending respectively. The setup was similar to the intended use as part of a hybrid structure and was conducted by constraining and ensuring the tape curvature was maintained at the root while incremental mass was applied to the tape tip. The tape springs in this experimental setup caused buckling to be offset by the constrained root. For completeness the steady state moments (M^*_-, M^*_+) are estimated at 28 Nmm and 52 Nmm respectively using an established and validated equation from Seffen and Pellegrino (1999) [36].

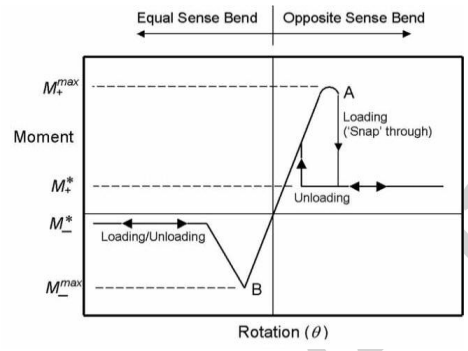

Fig. 5 Moment characteristics when bending a tape spring [25].

3. Experimental Setup and Development

The cantilever inflatable boom was attached at its root to a base plate by wrapping the nylon shell and rubber bladder around an inner plate of the same circumference as the boom. The join was sealed by an O-ring, and a collar was placed around the boom at the root to prevent any bulging from air pressure, providing a set root to define boom length. Figure 6 shows the completed setup of the boom, including the Nylon cord attached to the end plate providing a flat boom tip and attachment for the suspended weights. Figure 7 shows a schematic diagram of the boom root attachment.

Fig. 6 Setup of inflatable boom attached at base plate.

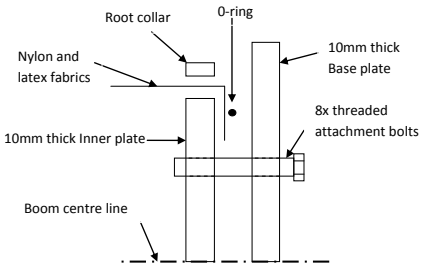

Fig. 7 Schematic of the boom root attachment.

Loads were applied by hanging weights at the tip of the boom causing a bending moment at its root. This was increased at 1 kg intervals between measurements and caused a tip deflection from which stiffness and bending moments were calculated. The deflections were measured by a height gauge capable of a 300 mm displacement range and accurate to within 0.01 mm. Measurements were taken optically using line of sight between the gauge and a marked centre of the boom end, resulting in a maximum underestimate of the boom deflection of 1 mm. To account for the change in the inflatable boom moment arm length under large deflections, the boom is assumed to rotate at its root allowing for tip deflection angle and hence moment arm to be estimated. Boom curvature from bending will cause this to be an underestimate, however for comparison between hybrid booms, deflections are expected to be moderate relative to the boom length and therefore errors small. The weights are accurate up to 0.5 g and the boom length was measured with a rule accurate to 1 mm. This resulted in the calculated bending moment being accurate to within ±0.14 Nm. The stiffness of the boom was calculated using the loading force applied and boom tip displacement values before buckling. The accuracy of the weights and deflection measurements resulted in a stiffness accuracy within 5%.

The boom tested with tape springs was manufactured to a length of 400 mm with a 50 mm radius, due to the ergonomics of handling the boom during setup. During preliminary studies, other boom lengths were also manufactured to assess any effects the length has on the boom performance. It was discovered that three important parameters need to be considered for the final optimum inflatable boom selection. These are: boom equilibrium, the warp direction and maximum tip deflections.

The equilibrium problem occurs because the inflatable boom is a soft system and will flex under loading. This causes the boom to behave in a quasi-static nature during tip deflection testing. This parameter, observed in the preliminary tests, showed that the booms do not reach equilibrium quickly and have a settling period of several minutes. It was found that the majority of the flexure happened in the first 5 minutes after each applied loading. Measurements taken within the first minute of the load being applied underestimated the deflection by up to 50 mm at boom buckling. It was found that displacement measurements taken at 1 minute after each applied load were a maximum of 4.4% from the displacements at equilibrium. This was less than the repeatability range of 5% (shown in Fig. 8) in the deflection data for these tests, and allowed the testing to be achieved on a suitable timescale. This preliminary testing took place at 69 kNm^{-2} (10 psig) using a 600 mm boom with no tape springs. It is intuitive that a structure stiffened through increased pressure or use of tape springs will reach equilibrium quicker, therefore reducing this error. This was confirmed as this effect was not easily observed in tests using shorter boom lengths or at higher inflation pressures. All subsequent tests, including those shown in Fig. 8, had tip deflection measurements taken at 1 minute after each incremental load was applied.

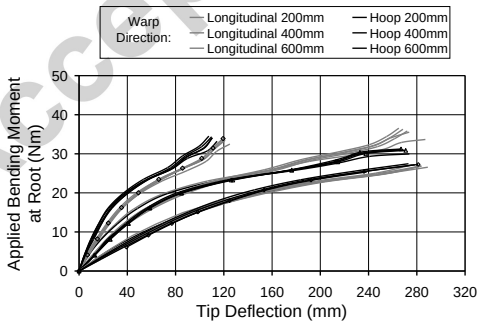

Fig. 8 Tip deflection data for 3 boom lengths and 2 fabric orientations for all repeat tests at 69 kNm^{-2}.

Figure 8 displays the tip deflection data for all 5 repeat tests for each boom length and fabric orientation tested at 69 kNm^{-2}. It highlights the spread in repeat results for each configuration confirming the averaged data is representative. For each data point there is a maximum of 5% in tip deflections between the repeat tests of each configuration. Figure 9 shows the averaged results of both 69 and 103 kNm^{-2} inflation pressures of the 200, 400, and 600 mm booms. Each boom had the warp yarns placed in both the hoop and longitudinal directions to determine any performance benefit in the orthotropic fabric. There is a slight performance advantage when using the warp in the hoop direction for the 200 mm boom. This is reduced as pressure and boom length are increased, where it becomes a disadvantage for 400 and 600 mm booms at various deflections, creating a less rigid structure. Due to the negligible differences in boom performance between the two orientations and the significant advantages of the tensile properties shown in the material testing section, the warp used in the hybrid boom testing was placed in the hoop direction to maximize the operating pressure.

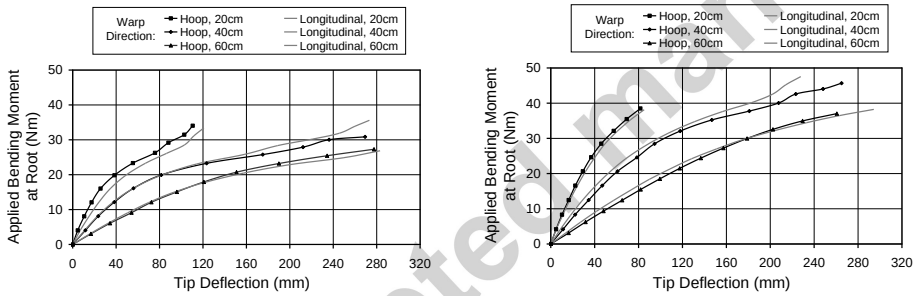

(a) 69 kNm^{-2} (b) 103 kNm^{-2}

Fig. 9 Averaged tip deflection data for 3 boom lengths and 2 fabric orientations.

The third observed parameter (maximum tip deflections) revealed, that for each of the preliminary boom lengths boom stiffness increases when the boom starts to impinge on the base plate representing a limitation of the test rig. This can be seen on some of the 200 and 400 mm boom deflection curves for tip deflections greater than 50% of the boom length. At this point any further deflection is not representative of the performance of the boom and testing was halted. The 600 mm boom could not be used in final testing as it is not possible to reach the buckling bending

moment within 300 mm of tip deflection, and could therefore not be accurately measured with the current height gauge.

In conclusion current experimental constraints limit the boom length to a maximum of 400 mm while taking test measurements after 1 minute. This ensures accurate repeatability of each test within a suitable accuracy for boom equilibrium. The warp yarns are placed in the hoop direction to maximise boom durability under inflation.

Analytical modeling of inflatable booms has been previously conducted across a wide range of permutations and as such is outside the scope of this paper. In addition it is not possible to implement isotropic models such as Comer – Levy as the fabric is a nonlinear orthotropic material. This was observed in the uniaxial UTS tests and has been investigated in detail in previous studies [37][38]. Further in depth study is required to accurately describe the fabrics material properties in the inflatable boom application and will be conducted in future investigations and applied to numerical models for both inflatable and hybrid booms. However an initial estimate of performance using Eqns. (1) and (2) can be performed for comparison against these inflatable booms.

The experimental inflatable boom results show that each boom tends towards a maximum bending moment of over 30 and 40 Nm for 69 and 103 kNm^{-2} inflation pressures respectively. However they are unable to achieve definitive maximum bending moments (M_{max}) due to experimental restrictions for tip deflections greater than 200 mm. The average radius of these booms was 52.5 ±0.4 and 53.3 ±0.5 for the two pressures respectively. Equation (1) gives a reasonable correlation to these results and predicts M_{max} values of 31.3 ±0.7 and 49.2 ±1.4 Nm for 69 and 103 kNm^{-2} respectively. This is supported by the observed incipient wrinkling moments, displayed in Fig. 10, being approximately half the predicted M_{max} values. This has been shown previously by Webber (1982) among others where differences to the experimental results can be attributed to the linearly elastic model of Eqns. (1) and (2) in comparison to the orthotropic fabric used in these inflatable booms. For the experimental inflatable booms the observed M_W is 16 and 26 Nm for these two inflation pressures respectively where the discreet tip loading intervals can account for an overestimation in their observation.

The change in radius at these inflation pressures from the constrained root and tip is significant and increases the structural capacity of theses booms. The predicted M_{max} values of Eqn. (1) are 27 and 41 Nm when considering a 50 mm boom at 69 and 103 kNm^{-2} respectively. Other stiffening effects must also be considered having been observed in highly inflated structures [16] and analysed in detail by Davids (2008). This is caused by work done by

pressure from deformation induced volume changes, such as boom bending and shearing, and can increase the structural capacity of inflatable booms beyond the $2M_W$ limit predicted by Comer and Levy. However to achieve these maximum bending moments would require large deflections and leave the inflatable boom too weak for the majority of applications. For comparison between the hybrid and inflatable booms failure limits are applied to quantify the performance advantage. The booms are deemed to have failed (M_{fail}) when wrinkling occurs on the inflatable boom at M_w. This also allows a direct comparison between boom rigidities taking the average stiffness of the booms up to this failure point prior to the considerable softening of the structure.

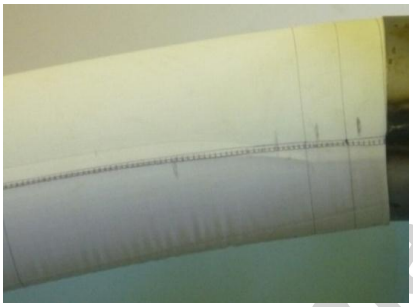

Fig. 10 Inflatable boom at 103 kNm^{-2} under 26 Nm showing wrinkling of the fabric.

When attaching tape springs to create a hybrid boom it is important to consider two factors in maximizing their stiffness: maintaining the no-slip condition between the boom and the tapes and the tapes' curvature. A tape securely attached to the boom will prevent any localized buckling of the fabric and increase the stiffness of the boom. This is because the compression strength of the tape spring is much greater than that of the boom, which is provided only by the internal pressure. This also results in a delayed buckling of the boom, increasing M_{fail}. Any slipping between the boom and the tapes will reduce this effect as the tape is not able to take the compressive loads. Flattening of the tapes will also reduce their maximum bending moments towards the steady state values, resulting in a stiffness reduction of the system. This research improves on the previous work by Walker et al (2011) [31], where tapes were held in place by pockets stitched into the boom. It has been shown that this setup allows some tape movement within the pockets, and flattens the tape due to the difference in radii between the boom and the tape with the inflation pressure. To satisfy both conditions and maximize the tape spring potential, this study used eight collars manufactured from 6 mm thick Perspex, as shown in Fig. 11.

The collars were glued at 48 mm intervals along the length of the boom, and a clamping system, shown in Fig. 12, attached the tapes at the root of the boom. The tape was also clamped at each collar, providing a fixed no-slip condition along the length, between the tape and the boom. The collars shown in Fig. 11 have been designed to be able to attach up to 12 tape springs around the circumference of the boom. This paper reports on the initial hybrid boom experimental investigations using up to 2 tape springs around the circumference of the boom. However future studies will fully utilize the collars with the multitude of possible hybrid boom configurations including varying the tape spring mass around the entire boom circumference. It is important to note that for each clamping point a 3 mm hole is punched out of the tape, potentially reducing the tape performance. The considerable disadvantages of the collar attachment system are the significant increase in mass and volume to the hybrid boom which limit its viability as a final design. Specifically as the framework structure is only collapsible into a zigzag pattern where voids in the stowed boom will cause significant packing inefficiencies with respect to a rolled up design. A final solution would likely attach the tape springs directly onto the inflatable boom with a suitable adhesive allowing the structure to be rolled onto a mandrel preventing voids and maintaining the significant packing efficiencies of inflatable structures.

Although not suitable as a final design, the collar attachment method is selected for initial structural analysis. It is used in the following studies as it is a simple system that can be modified easily for testing various tape spring configurations whilst minimizing time and resources and maximizing the number of tested permutations.

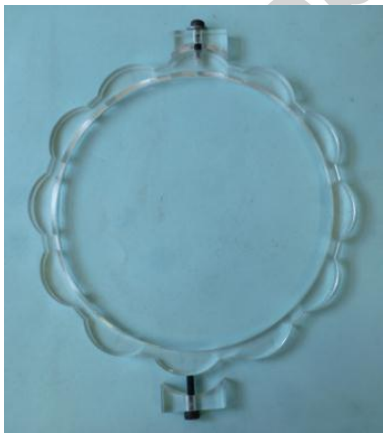

Fig. 11 Tape spring supporting collar. **Fig. 12 Tape spring root clamping assembly.**

Table 2 shows the mass of the hybrid boom in its component parts. The mass of the inflatable boom (Nylon shell, bladder, and tip end plate and cord) is 135 g, which is the test boom mass. The 400 mm inflatable boom mass is increased by 17 g when adding two tape springs. This mass is increased by a further 165 g when the eight collars and clamping devices are added. The collars are placed at 45 mm intervals along the length of the boom, totaling 317 g for the test mass of a hybrid boom with two opposed tape springs attached. This increases the mass of the inflatable system by 2.4 times the original mass. The majority of the added mass comes from the collar–clamping system used. The percentage mass increase added by the tapes is 13%.

Alternative preliminary attachment methods included the use of pockets, gluing tapes directly to booms, and simply clamping them at either end of the boom. However the collar attachment setup created the stiffest hybrid boom and maximised the structural performance benefit of the tape springs. Although this setup is not a final attachment design it provides an excellent starting point to determine overall trends of hybrid booms.

Table 2 Mass breakdown of the hybrid boom components.

Boom component	Mass
Nylon shell	16.2 g
Bladder	66.3 g
Tip end plate	52.3 g
Weight attachment cord	0.5 g
Tape spring	8.5 g
(per) Tape spring root assembly	8.9 g
(per) Tape spring collar	14.0 g
(per) Collar attaching clamp	2.2 g

The boom testing can be split into two parts; inflatable boom testing, and hybrid boom testing, where Fig. 13 shows the various test configurations. All the testing, unless otherwise stated, was undertaken at both 69 kNm^{-2} (10 psig) and 103 kNm^{-2} (15 psig). For each inflation pressure, the inflatable boom (configuration A) had five repeat tests. From this structure a hybrid boom was assembled and tested in various orientations. The hybrid boom testing was split into a further two sections; two opposed tape springs (configurations B, C, D), and doubled tape springs (configurations E, F). The opposed tape spring orientation used two tape springs placed on opposite sides of the boom and was chosen for ease of comparison between previous experiments [31]. It was also the most likely setup

to provide maximum stiffness to the structure using only 2 tape springs which could be confirmed with testing configurations E and F. The opposed tape pair was tested in three orientations in relation to the direction of the applied load. These were:

- A tape pair vertically aligned with the applied load (configuration B)
- A tape pair at 45^0 to the applied load (configuration C)
- A tape pair horizontally aligned with the applied load (configuration D)

These are illustrated in the cross sectional diagram of Fig. 13. This forms the main focus of this paper, with tip deflection testing allowing us to evaluate the structural performance change when altering the second moment of area of the hybrid boom. The selected attachment system to create this hybrid boom is a framework structure which has its own inherent stiffness exclusive of the inflatable boom. To assess the performance of this created framework structure testing in configurations B, C, and D was undertaken at an additional pressure of 0 kNm^{-2}. This also gives an indication on the structural performance of the hybrid boom if inflation pressure was not maintained. A pressure leak from material degradation or a puncture from micro meteorites are typical examples in space applications and is an advantage over inflatable booms which must consider the cost of maintaining long term rigidisation. The range of inflation pressures tested at will give an indication of the performance trends of these structures. Three repeat tests were completed for each of the 3 inflation pressures and 3 tape spring orientations, which resulted in 27 individual tests for the opposed tape pair testing.

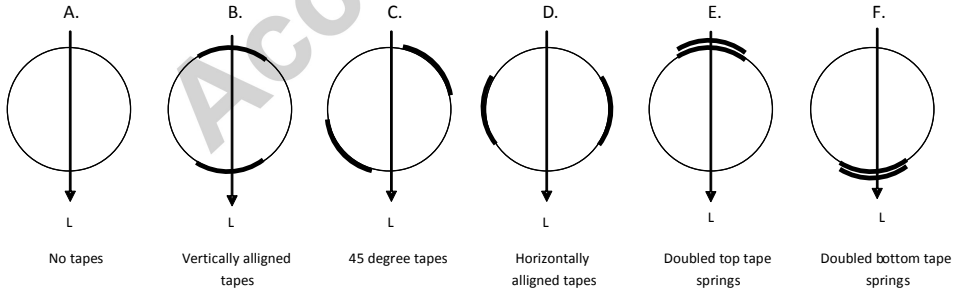

Fig. 13 Cross-section of test configurations with direction of the applied load, L.

To explore tape location in more depth and identify the optimum placement of two tape springs doubled tape spring testing of configurations E and F was conducted at 69 kNm^{-2} (10 psig). 3 repeat tests for 2 tape spring orientations gave a total of 6 individual tests for the doubled tape spring configurations. This gave a total of 10 tests for the inflatable boom experiments, and 33 tests for the hybrid boom, totaling 43 individual tests for comparison between inflatable and hybrid booms.

4. Experimental Results and Discussion

Figure 14 displays the applied bending moment and resultant deflections of the booms at 69 and 103 kNm^{-2} respectively for configurations A-D. The increased structural stiffness and buckling moment the hybrid booms can achieve is seen immediately and is most rigid when the pair of tape springs are placed in configuration B. These deflect up to a maximum of 40 mm prior to boom failure for a maximum applied bending moment of 52 Nm at 69 kNm^{-2} inflation pressure. When rotating the orientation of the opposed tape springs towards the horizontal alignment in configuration D, the stiffness of the boom reduces.

This also reduces the average buckling bending moment from 41 Nm to 28 Nm at 69 kNm^{-2}. This result is expected, as the second moment of area of the tape springs on the boom in the loading axis is reduced from 3.561 to 0.043 cm^4 for configurations B and D respectively, and should be maximized to achieve the most rigid structure. All tests of configuration C result in boom rigidity and buckling moment values between configurations B and D. This follows the trend of the reduction in the hybrid boom's second moment of area, resulting in a reduction in structural performance. As you would expect, due to the altered second moment of area, there is also lateral deflection when the opposed tapes are placed in configuration C, resulting from 3D torsional bending of the tape springs. The behaviour of a tape bending in 3 dimensions has been investigated in detail by Walker et al 2007 [25]; however, this falls outside of the scope of this paper and therefore the sideways deflections were not measured.

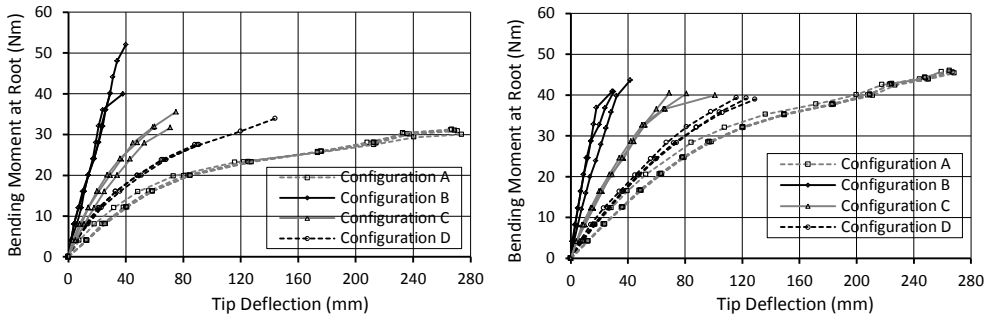

(a) 69 kNm^{-2} (b) 103 kNm^{-2}

Fig. 14 Tip deflection data for applied bending moments.

The vertically aligned tape springs in configuration B buckle like a hinge. This happens suddenly at the boom root, and can be seen by the abrupt change in boom stiffness in some of the deflection curves. Unlike the vertically aligned tapes in configuration B, Figure 15 shows that the opposed tapes in configuration D behave similarly to a simple cantilever beam. The resultant tension and compression stresses across the tape width cause the tape springs to buckle in on themselves. This tape spring failure occurs gradually as tip mass is applied, and is mirrored by the deflection curve data. Similarly to the inflatable boom the hybrid boom failure limit is set at M_W where an averaged boom rigidity up to this point allows for a direct comparison between all inflatable and hybrid boom configurations. Configuration D provides 22% additional stiffness to an inflatable boom at 103 kNm^{-2}. This is significantly lower in comparison to the performance of configuration B that can provide over 4.2 and 4.9 times at 69 and 103 kNm^{-2} respectively.

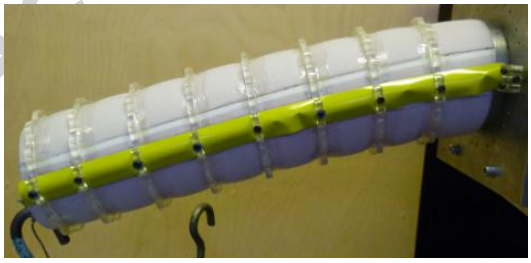

Fig. 15 Configuration D at 32.8 Nm applied bending moment at root under 103 kNm^{-2}.

The framework structure created by the attachment collars and tape springs have their own inherent structural performance. This was investigated by testing the hybrid boom at 0 kNm^{-2} inflation pressure with the tip deflection results shown in Fig. 16. This shows that the framework structure created by the collars and two tape springs can maintain up to a 13 Nm applied bending moment without buckling when using configuration B. Comparing this setup to configuration A at 103 kNm^{-2} shows a 53% reduced initial structural rigidity, for a 35% increase of mass. The maximum bending moment is also reduced significantly to 3 and 1 Nm for configurations C and D respectively, where the hybrid boom is rotated to 45 degrees and horizontal tape spring alignments. The average stiffness of configuration B drops from 4.06 to 3.26 and 0.39 kN/m for internal pressures of 103, 69 and 0 kNm^{-2} respectively.

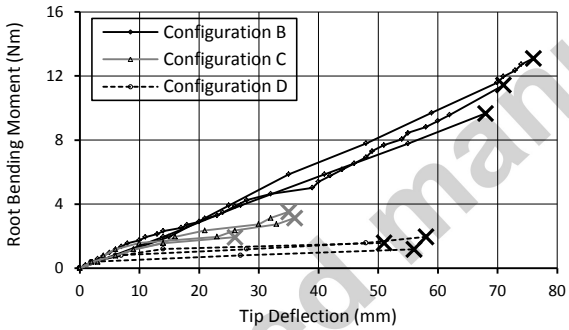

Fig. 16 Tape spring stiffness at 0kNm^{-2}.

The results of the opposed tape spring testing in configurations B, C and D indicates that maintaining tapes in their optimum stiffness orientation of configuration B and maximizing the second moment of area, offers the greatest structural performance. A further test programme was undertaken to explored in more depth and identify the most effective position two tape springs can be located. Two tapes were placed on either the top or bottom surfaces of the boom in separate test cases (configurations E and F), at an inflation pressure of 69 kNm^{-2} (10 psig). All other setup and test procedures remained the same. These tape configurations were chosen as tapes placed out of alignment with the applied load, such as in configurations C and D, experience a reduction in structural performance.

Figure 17 shows all the repeat deflection data for configurations E and F, with previous data from configurations A and B for comparison.

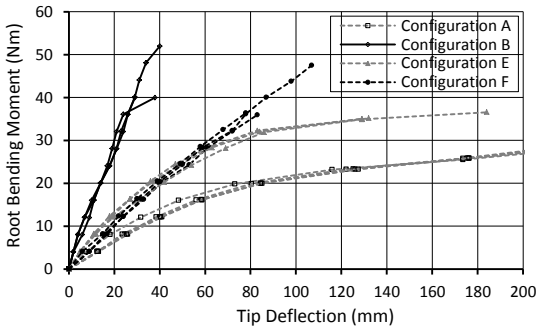

Fig. 17 Doubled tape spring comparison deflection data at 69 kNm^{-2}.

Figure 17 illustrates that doubling up tape springs on one side of a hybrid boom can maintain an average failure bending moment of 32 and 40 Nm for configurations E and F respectively. The average stiffness for configurations E and F are 1.18 and 1.13 kN/m respectively. Configuration F, like B, tends to deflect linearly until the tapes buckle. Although having a slightly lower rigidity, configuration F provides a stiffer boom for applied bending moments above 20 Nm in comparison to configuration E. This is expected, as the tapes in configuration F are subjected to opposite sense bending in compression. This improves the inflatable boom two fold, as fabrics cannot withstand compressive forces, and it utilizes the stronger tape orientation. The data then stops abruptly as during testing the tape springs failed catastrophically, with permanent deformation and tearing as soon as the next incremental load was applied. This led to sudden large tip deflections of over 100 mm, and for safety and longevity of the boom the experiment was stopped. In contrast, for configuration E, where tapes were placed on the top surface only, buckling occurred cleanly and the tapes were not permanently deformed. This meant that the tapes continued to provide some additional stiffness to the boom, as shown by the gradual flattening of the gradient in the deflection data seen in Fig. 17.

Although the failure bending moment of configuration F is comparable, it is clear from Fig. 17 that there is a considerable increase in stiffness of over 2.9 times when placing two opposed tape springs in configuration B. This confirms the use of a pair of tapes placed on opposite sides of the boom as the most effective for simple single

unidirectional loading cases. It also shows that placing a pair of tapes on each side of the boom, providing both compressive and tensile support to the boom, maximises the boom's rigidity. Configuration B could be acting similarly to a composite beam whereby the top tape is acting as a tie between to the inflatable boom through the collars while the bottom tape acts as a compressive strut. This is because the tapes and collar attachment system creates a framework structure down the length of the boom in configuration B. This framework has its own rigidity as shown by Fig. 16 and is created by the separation between the two tapes. Even though one tape is placed in the weaker equal sense bend orientation in configuration B, the separation moves the stiffest part of the structure away from the neutral axis and results in a far stiffer boom. Configurations E and F result in a neutral axis significantly closer to the tapes resulting in a much smaller second moment of area giving a significantly less rigid boom, albeit with both tapes placed in the stronger opposite sense orientation. Therefore equal priority must be given to tapes on both top and bottom surfaces to further improve the hybrid boom performance.

Table 3 Average boom performance in various configurations (* peak values).

Boom configuration (with boom masses)	Pressure (kNm^{-2})	M_{fail} (Nm)	Averaged stiffness (kN/m)
A [No Tapes]	69	16	0.78
(135 g)	103	25	0.83
B [Vertically aligned tapes]	0	11	0.39
(317 g)	69	41*	3.26
	103	39	4.06*
C [45 Degree tapes]	0	3	0.24
(317 g)	69	32	1.54
	103	37	1.63
D [Horizontally aligned tapes]	0	2	0.08
(317 g)	69	28	0.99
	103	32	1.01
E [Doubled top tapes]	69	32	1.18
(299 g)			
F [Doubled bottom tapes]	69	40	1.13
(299 g)			

Table 3 gives the results of the average failure bending moments and stiffness's for the various boom configurations with their corresponding boom masses. It shows that adding tapes springs increases the average stiffness of the inflatable boom by up to 4.9 times when two opposed tapes are added in configuration B (vertically aligned tapes), from 0.83 to 4.06 kN/m at 103 kNm^{-2} inflation pressure. Adding two opposed tapes increases the

mass of the system by 2.4 times. The boom is most rigid when at 103 kNm^{-2} inflation pressure but shows a slight decrease of 5% in maximum bending moment when compared to the lower inflation pressure of 69 kNm^{-2}. This is the same as the 5% spread in the repeat testing and could be attributed to slight variations and defects in the tape springs which can lead to significant changes in peak bending moments [25]. This suggests the buckling moment limit for the tape springs in configuration B is a maximum of approximately 41 Nm where increased pressure increases boom rigidity only. Further repeat testing and testing at higher and lower pressure intervals is required to establish if this is a trend and provide greater detail to this system.

A tradeoff occurs in inflatable boom performance between using tape springs or using fabric materials (resulting in an increased operating pressure), to achieve maximum stiffness and bending moment for minimum boom mass. This will be achieved in future research by investigating a wider range of operating pressures and fabric and tape spring thicknesses. Nonetheless, this research has shown that attaching a pair of tape springs in their most efficient orientation (configuration B) will increase the rigidity and buckling bending moment of the hybrid boom significantly and, proportionally, much more than the mass added to the system for the pressures tested.

5. Conclusions and Further Research

This paper shows that the use of tape springs as structural stiffeners, added to an inflatable boom to create a hybrid structure, improves the structural performance. Tip deflection testing of the inflatable and hybrid boom was undertaken at three inflation pressures; 0, 69, and 103 kNm^{-2}, with the hybrid boom tested in 5 tape spring configurations. For the inefficient (in terms of mass added) tape spring attachment system used, it has been shown that the hybrid structure increases the failure bending moment and the initial rigidity of an inflatable boom by up to 4.2 and 4.9 times respectively. This is for a mass penalty of 2.4 times the starting mass. Studies into the orientation and placement of a pair of tape springs confirm that two placed on opposite sides of the boom, inline with the applied load, offers the maximum performance to the hybrid boom of 41 Nm buckling bending moment and 4.06 kN/m initial rigidity. The attachment system for the tape spring to the boom improves on previous work by maintaining tape curvature and ensuring a non-slip condition between tape and boom. This can be seen in the increase in buckling bending moments between this paper and Walker et al (2011) [31] of 41 and 25 Nm respectively, whilst using the same boom materials, setup and inflation pressures. The attachment mechanism

presented here is not a final design as it contributes the majority of the added mass to the hybrid structure and will significantly affect the stowage and deployment performances not considered in this paper. However this investigation of hybrid booms has provided an excellent initial system to achieve rapid testing over a range of permutations from which to build on in future research.

Further testing will be undertaken considering the many permutations of tape springs mass placement with respect to circumferential location including using four tape locations in a cross configuration. This is a likely setup for general applications with more complex loading profiles. Analysis into this cross configuration setup will investigate the off-design performance of the structure to determine the overall performance of the hybrid boom for space applications. Additionally future research will aim to model these hybrid structures with respect to structural performance giving a greater insight into the load-deflection response of these booms. Future hybrid boom research is needed for the detailed analysis of stowage performance with respect to the tradeoff against other performance criteria, and the development and test of hybrid boom deployment systems. The performance of hybrid booms in both these areas will be highly dependent on the attachment system and will demand the development of a suitable tape spring attachment. This technology is highly flexible where tape spring placement can be tailored for peak moment and rigidity performance optimisation. To achieve this existing inflatable boom models require a detailed understanding of the nonlinear orthotropic fabric material properties from which the isotropic reinforcing tape springs can be added to create a composite system in a similar manner as presented by Brayley et al. (2012).

It can be concluded that using tape springs to create a hybrid boom can significantly increases the rigidity and buckling bending moments of an inflatable boom. The optimum placement of these tapes for maximum structural performance of the boom is found to be on opposing sides, inline with the applied load. The tapes and attachment mechanism also creates a framework that can still maintain some structural performance when under no inflation pressure, providing an added advantage over traditional inflatable structures.

References

[1] Futron corporation, "Space Transportation Costs: Trends in Price per Pound to Orbit 1990-2000," Bethesda, Maryland, USA, Sept 6, 2002, URL: http://www.futron.com/pdf/resource_center/white_papers/FutronLaunchCostWP.pdf [cited 11 Oct 2011].

Formatted: Font color: Auto

[2] de la Fuente, H., Raboin, J., Spexarth, G., and Valle, G., "TransHab: NASA's large-scale inflatable spacecraft," *Proceedings of the 41st AIAA/ ASME/ASCE/AHS/ASC Structures, Structural Dynamics, and Materials Conference*, AIAA, Apr 3-6, Atlanta GA, USA, 2000, pp. 1-9.

[3] Messerschmid, E. W., and Renk, F., "Space Stations," Encyclopedia of Aerospace Engineering, John Wiley & Sons, Ltd, Hoboken, 1st ed., Dec. 15, 2010, Chap 2, URL: http://onlinelibrary.wiley.com/doi/10.1002/9780470686652.eae424/full [cited 11 Oct 2011].

[4] Foust, J. "Bigelow still thinks big," *The Space Review*, 2010, Nov. 1, URL: http://www.thespacereview.com/article/1719/1 [cited 11 Oct 2011].

[5] Peypoudat, V., Defoort, B., Lacour, D., Brassier, P., Couls, O.L., Langlois, S., Lienard, S., Bernasconi, M., and Gotz, M., "Development of a 3.2m-long inflatable and rigidizable solar array breadboard," 46th AIAA/ASME/ASCE/AHS/ASC Structures, Structural Dynamics & Materials Conference, Austin, TX, Apr 18-21, 2005.

[6] Malone, P.K., and Williams, G.T., "A Lightweight Inflatable Solar Array," Proceedings of the 9th Annual AIAA/USU Conference on Small Satellites, AIAA, Washington, DC, 1995.

[7] Cui, D., Yan, S., Guo, X., Chu, F., "An overview of dynamics modeling of inflatable solar array," Energy Procedia, pp. 1967-1972, Vol. 14, 2012.

[8] Pacini, L., Kaufman, D., Adams, M., Lou, M., and Carey, J., "Next Generation Space Telescope (NGST) Pathfinder Experiment, Inflatable Sunshield in Space (ISIS)," *Proceedings of a conference held at Hyannis*, ASP Conference Series, edited by E. P. Smith, and K. S. Long, Vol. 207, Next Generation Telescope Science and Technology, Hyannis, MA, Sept. 13-16, 1992, pp. 365-375.

[9] Lou, M., "Development and application of space inflatable structures," Proceedings of the 22nd International symposium on space technology and science, ISTS, Morioka, Japan, pp. 537-545, May-Jun 28-4, 2000.

[10] Leonard, R., and Brooks, G., "Structural considerations of inflatable re-entry vehicles," NASA TND-457, Sept, Los Angeles, USA, 1960.

[11] Comer, R. L., and Levy, S., "Deflections of an Inflatable Circular Cylinder Cantilever Beam," *AIAA Journal*, Vol. 1, Jul, 1963, pp. 1652–1655.

[12] Webber, J. P. H., "Deflections of Inflated cylindrical cantilever beams subjected to bending and torsion," *Aeronautical Journal*, Vo. 86, Issue 858, Oct. 1982, pp. 306-312.

[13] Main, J.A., Peterson, S.W., and Strauss, A.M., "Beam-type bending of space-based inflated membrane structures," *Journal of Aerospace Engineering*, Vol. 8, No. 2, pp. 120-125, Apr, 1995.

[14] Veldman, S.L., Bergsma, O.K., and Beukers, A., " Bending of anisotropic inflated cylindrical beams," *Thin-Walled Structures*, Vol. 43, No. 3, pp. 461-475, 2005.

[15] Veldman, S.L., "Wrinkling prediction of cylindrical and conical inflated cantilever beams under torsion and bending," *Thin - Walled Structures, Vol. 44, No. 2*, pp. 211-215, *Feb*, 2006.

[16] Thomas, J.C., and Wielgosz, C., "Deflections of highly inflated fabric tubes," *Journal of Thin-Walled Structures*, Vol. 42, pp. 1049-1066, 2004.

[17] Davids, W.G., "Finite-element analysis of tubular fabric beams including pressure effects and local fabric wrinkling," *Finite Element in Analysis and Design*, Vol. 44, No. 1-2, pp. 24-33, Dec, 2007.

[18] Davids, W.G., and Zhang, H., "Beam finite element for nonlinear analysis of pressurized fabric beam-columns," *Engineering Structures*, Vol. 30, pp. 1969-1980, 2008.

[19] Du, Z., Tan, H., and Wang, C.G., "Wrinkling characteristic of membrane inflated truncated cone," *Proceedings of the 18th International Conference on Composite Materials*, Edinburgh, U.K, Jul 27-31, 2009.

[20] Davids, W.G., "In-plane load-deflection behaviour and buckling of pressurized fabric arches," *Journal of Structural Engineering*, Vol. 135, pp. 1320-1329, Nov, 2009.

[21] Tamadapu, G., and DasGupta, A., "Finite inflation analysis of a hyperelastic toroidal membrane of initially circular cross-section," *International Journal of Non-Linear Mechanics*, Vol. 49, pp. 31-39, 2013.

[22] Wang, C., Tan, H., Du, X., and He, X., "A new model for winkling and collapse analysis of membrane inflated beam," *Acta Mechanica Sinica*, Vol. 26, No. 4, pp. 617-623, May, 2010.

[23] Brayley, K.E., Davids, W.G., and Clapp, J.D., "Bending response of externally reinforced inflated braided fabric arches and beams," *Construction and Building Material*, Vol. 30, pp. 50-58, 2012.

[24] Lou, M., Fang, H., and Hsia, L., "A Combined Analytical and Experimental Study on Space Inflatable Booms," *IEEE Aerospace Conference Proceedings*, IEEE, Vol. 2, Big Sky, Montana, March, 2000, pp. 503-512.

[25] Walker, S.J.I., and Aglietti, G.S., "Modelling the hinge moment of skew-mounted tape spring folds," *Journal of Aerospace Engineering*, Vol. 20, No. 2, pp. 102-115, 2007.

[26] Johnson, L., Whorton, M., Heaton, A., Pinson, R., Laue, G., and Adams, C., "NanoSail-D: A solar sail demonstration mission," *Acta Astronautica*, Vol. 68, No. 5-6, pp. 571-575, Mar-Apr, 2011.

[27] Biddy, C., Alford, C., Bertino, M., Diaz, A., Nehrenz, M., and Svitek, T., " Challenges and design of Lightsail-1 boom deployment module," *Proceedings of the 2nd International Symposium on Solar Sailing*, New York City, NY, Jul 20-22, 2010, pp. 87-90.

[28] Lappas, V., Adeli, N., Visagie, L., Fernandez, J., Theodorou, T., Steyn, W., and Parren, M., "CubeSail: A low cost CubeSat based solar sail demonstration mission," *Advances in Space Research*, Vol. 48, No. 11, pp. 1890-1901, Dec 1, 2011.

[29] Watt, A.M., and Pellegrino, S., "Tape - spring rolling hinges," *Proceedings of the 36th Aerospace Mechanisms Symposium*, Cleveland, OH, pp. 1-14, May 15-17, 2002.

[30] Walker, S.J.I., Kiley, A., Aglietti, G.S., Cook, A.J., and McDonald, A.D., "Modelling Three Dimensional, Tape Spring Based, Space Deployable Structures," *Proceedings of the 12th European Conference on Spacecraft Structures, Materials and Environmental Testing*, Noordwijk, Netherlands, Mar 20-23, 2012.

[31] Walker, S. J. I., McDonald, A. D., Niki, T., and Aglietti, G. S., "Initial performance assessment of hybrid inflatable structures," *Acta Astronaut*ica, Vol. 68, Issues 7-8, April-May, 2011, pp. 1185-1192.

[32] Block, J., Straubel, M., Wiedemann, M., "Ultralight deployable booms for solar sails and other large gossamer structures in space," *Acta Astronautica*, Vol. 68, Issues 7-8, April-May, 2011, pp. 984-992.

[33] "Fibremax Stabilized Nylon," Challenge Sailcoth Sales Brochure, 2009.

[34] Megson, T. H. G., *Structural and stress Analysis*, 2nd ed., ELSEVIER Butterworth-Heinemann, Oxford, UK, 2005, Chap. 7.

[35] British Standard Aerospace Series, "Inspection and testing of textiles for aerospace purposes", BS 6F 100:1998, Feb. 2008.

[36] Seffen, K. A., and Pellegrino, S., "Deployment dynamics of tape springs," *Proceedings of Mathematical, Physical and Engineering Sciences*, Published by The Royal Society, London, Vol. 455, Mar. 8, 1999, pp. 1003-1048.

[37] Hutchings, A.L., Braun, R., Masuyama, K., Welch, J.V., "Experimental determination of material properties for inflatable aeroshell structures," *Proceedings of the 20th AIAA Aerodynamic Decelerator Systems Technology Conference and Seminar*, AIAA-2009-2949, Seattle, WA, May 4-7, 2009.

[38] Apedo, K.L., Ronel, S., Jacquelin, E., Bennani, A., and Massenzio, M., "Nonlinear finite element analysis of inflatable beams made from orthotropic woven fabric," *International Journal of Solids and Structures*, Vol. 47, pp. 2017-2033, Apr, 2010.

[39] Freeland, R.E., Bilyeu, G.D., Veal, G.R., and Mikulas, M.M., "Inflatable deployable space structures technology summary," *49th International Astronautical Congress*, IAF-98-I.5.01, Melbourne, Australia, Sept-Oct 28-2, 1998.

[40] Maessen,D., "Development of a generic inflatable de-orbit device for CubeSats," *Proceeding of the 58th International Astronautical Congress*, IAC-07-A6.3.06, May, Hyderabad, India, Sept, 2007.

Fig. 1 Setup of the nylon tensile testing.

Fig. 2 Uniaxial tensile $\sigma - \varepsilon$ data of the Fibremax 94 Nylon fabric.

Fig. 3 Over pressurisation failure at 165 kNm^{-2} of a 50 mm radius inflatable fabric boom.